*Structural Engineering and Mechanics, Vol. 10, No. 5 (2000) 505-516*
DOI: http://dx.doi.org/10.12989/sem.2000.10.5.505


# Inelastic behavior of standard and retrofitted rectangular hollow sectioned struts. II: Experimental study

Medhat Boutros†, James McCulloch‡ and Damian Scott‡

*The University of Western Australia, Nedlands 6907, Australia*

**Abstract.** This paper is a presentation of an experimental study about the elastic-partly plastic behavior of rectangular hollow steel pinned struts subjected to static cyclic axial loading and the evaluation of the compressive strength of retrofitted crooked struts. Retrofitting is achieved by welding stiffening plates along the webs of damaged struts. The material follows a quasi-kinematic hardening hysteresis path as observed from coupon tests. Test results are compared to those of an analytical model showing a good agreement for both standard and retrofitted struts. The comparison of different stiffener plate dimensions shows that more efficient strengthening is achieved by using long thin stiffeners rather than short thick ones.

**Key words:** bracing; compressive strength; cyclic loads; hysteresis; partial plasticity; retrofitting; steel; struts; testing.

## 1. Introduction

Empirical models of the hysteretic behavior of struts (e.g., Jain *et al.* 1978) were developed by piecewise linearisation of experimental observations. These tests were performed on inclined bracing members mounted through gusset plates on a loading frame. The response of the braces in these tests reflected the effects of the stiffness and strength of the gusset connections.

In this paper, quasi-static cyclic tests on pinned rectangular hollow section (RHS) struts are presented. The material hysteretic properties are determined on the basis of test observations and considered in the analysis of the struts.

An analytical model was developed for the reponse of struts accounting for partial plasticity, geometric nonlinearity and hysteretic material properties.

In the following section, the mathematical model of material properties is discussed. Then, the test apparatus is described. The following two sections are the comparison of the model with test results for undamaged struts and retrofitted damaged struts and an assessment of the efficiency of retrofitting alternatives. Finally, general conclusions are summarised.

† Formerly, Lecturer
‡ Graduates

## 2. Material properties

Static tests under axial cyclic loading performed on clamped 500 mm full RHS coupons showed that the material softened gradually from the initial (elastic) constant stiffness to a final (strain hardening) almost constant stiffness at a strain of about three times the (nominal) yield strain (Fig. 1). This behavior included the effects of residual stresses and strains due to manufacturing of the hot formed tubes. This inelastic material stiffness may be represented by:

$$\left.\frac{\partial\sigma}{\partial\varepsilon}\right|_{\sigma>\sigma_y^c} = \left[\lambda+(1-\lambda)e^{-\left(\frac{\varepsilon-\varepsilon_y^c}{\varepsilon_r}\right)}\right]E \tag{1}$$

Then, by integration:

$$\sigma|_{\sigma>\sigma_y^c} = \sigma_y^c + \left[\lambda(\varepsilon-\varepsilon_y^c)+\varepsilon_r(1-\lambda)\left(1-e^{-\left(\frac{\varepsilon-\varepsilon_y^c}{\varepsilon_r}\right)}\right)\right]E \tag{1a}$$

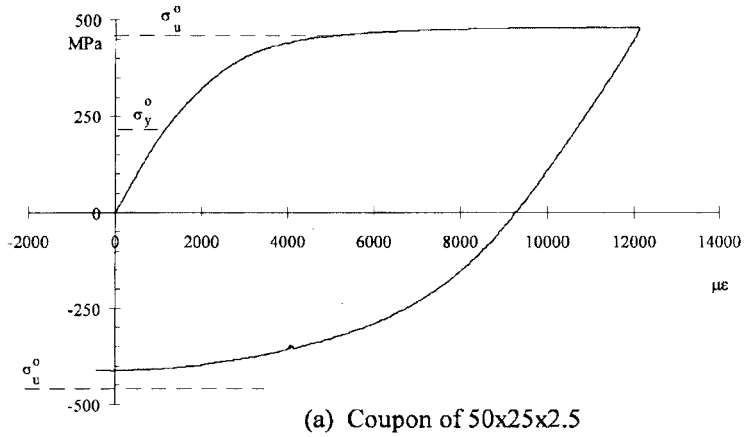


(a) Coupon of 50x25x2.5

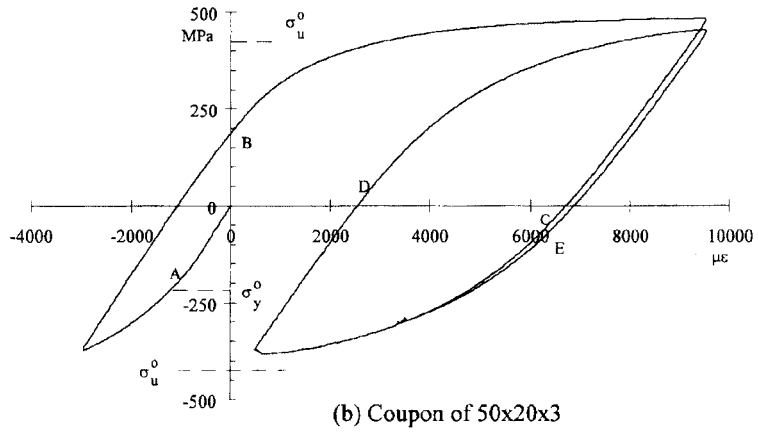


(b) Coupon of 50x20x3

Fig. 1 Stress-strain relations of RHS coupons

where $$\varepsilon_y^c=\frac{\sigma_y^c}{E}, \qquad \varepsilon_r=\frac{\sigma_u^o-\sigma_y^c}{\sigma_y^o}\varepsilon_y^o \tag{1b}$$

and $\lambda$ is the asymptotic slope of the final inelastic stress-strain relation as a proportion of the elastic stiffness $E$. During a given stroke and at a given fibre, $\sigma_y^c$ is the yield stress (end of linear stage) for the current stroke, $\varepsilon_y^c$ is the yield strain increment for the current stroke (taking the stress-free condition as reference) and $\varepsilon_r$ is a reference strain. $\varepsilon_y^o$ and $\sigma_y^o$ are the initial (nominal) yield strain and stress of the material and $\sigma_u^o$ is the nominal ultimate stress defined as the onset of the straight segment of the plastic stress-strain relation. The origin of Eqs. (1) is located at the point of zero stress of the corresponding stroke.

The responses in Fig. 1 show that the cyclic yield stress $\sigma_y^c$ exhibits kinematic softening with a constant total linear portion more than twice the nominal yield stress $\sigma_y^o$. However, the ultimate stress is almost constant. This "quasi-kinematic" effect is accounted for in the expression of the stresses (Eq. 1) by means of $\varepsilon_r$ which was set to produce a higher strength recovery (plastic stress increment) for lower values of $\sigma_y^c$ so as to maintain a constant ultimate stress. Coupon tests also showed that the elastic stroke at unloading from a plastic state was larger than $2\sigma_y^o$ after a short yield stroke such as at unloading from the first compression for the 50×20×3 coupon (Fig. 1b). The linear segment approached $2\sigma_y^o$ after a large plastic strain as per the later strokes of the same coupon. This is clear from the length of the straight line ending at point B which is larger than those ending at C, D and E. The later linear strokes are about $2\sigma_y^o$. Also, the lengths of the straight segments ending at E and C, after unloading from similar stresses, are almost equal even though the first was preceded by a larger plastic stroke. This suggests that the lengths of the linear segments are more dependant on the level of stresses than on the magnitude of previous plastic strains.

Therefore, the material was assumed to follow a quasi-kinematic hardening stress path as shown in Fig. 2. The cyclic hardening stress for the current plastic state was taken as a lower curve similar and asymptotic to Eq. (1a):

$$\sigma_y^h\Big|_{\sigma>\sigma_y^c}=\sigma_y^o+\left[\lambda(\varepsilon-\varepsilon_y^o)+\frac{\sigma_u^o-\sigma_y^o}{\lambda_y E}(\lambda_y-\lambda)\left(1-e^{-\left(\frac{\lambda_y E(\varepsilon-\varepsilon_y^o)}{\sigma_u^o-\sigma_y^o}\right)}\right)\right]E\le\sigma^c \tag{2}$$

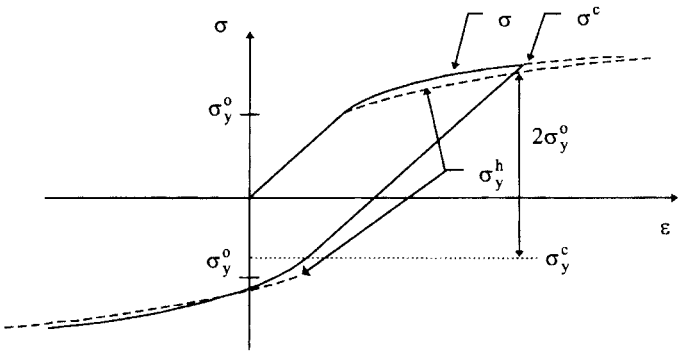


Fig. 2 Hysteretic stress-strain model

where $\lambda_y$ is a dimensionless hysteresis parameter and $\sigma^c$ is the inelastic stress reached before unloading. Upon unloading from a yield stage, the material returns to linear elasticity until it yields in the opposite direction. The elastic stroke between the two yield stresses, $\sigma_y^h$ at the end of the previous stroke and that at first yield in the unloading stroke, is $2\sigma_y^o$. The two functions in Eqs. (1a) and (2) are asymptotic at infinite strain thus replicating the observations about Fig. 1(b). It was shown (Boutros 2000) that the results of the analysis are sensitive to the value of the current yield stress (start of the nonlinear relation).

The hysteretic decrease in elastic stiffness is apparent in the coupon tests with a decrease of up to 10% (Fig. 1). In the strut analysis, a uniform value of the modulus of elasticity $E$ was used irrespectively of the position along and across the strut. A cyclic decrease of 1% per stroke was considered in average over the whole strut.

## 3. Test apparatus

The testing configuration is shown in Fig. 3. Similar smaller pinned end pieces were previously developed by Nonaka (1989). Longitudinal deformation was measured by two displacement transducers mounted on straight arms between the centers of the pins. Midspan deflection was measured using two lateral displacement transducers. The specimens were tested on an Instron loading frame. The end pins were lubricated and the weight of the moving heads was balanced using lead counterweights to minimise end moments. However, a small friction at the pins seems to have restrained the rotation about the pins and delayed the deformation of the specimens. For example, Fig. 4(a) of the test results for an RHS 50×20×3 shows compression peaks followed by a sudden drop at a small midspan deflection. The magnitude of the drop decreased with cyclic

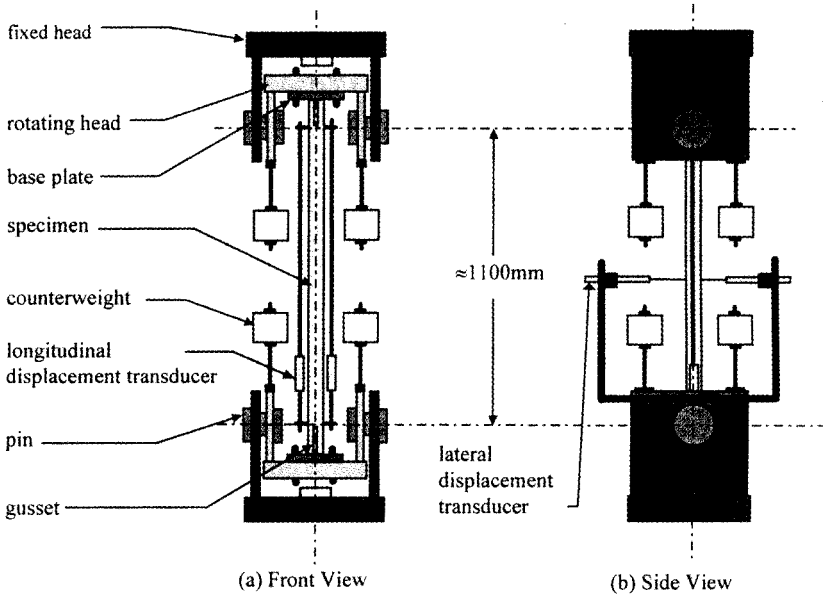


Fig. 3. Test configuration

loading due to the increase in lateral deflection resulting in larger moments at the pins. Initially the specimen was almost straight. As the midspan deflection increased in later cycles, the end moment increased and the friction at the pins could be more easily overcome. Note that these steep peaks are absent in the analysis (Fig. 4). Also, at unloading from tension, a sudden change in lateral deflections was recorded (Fig. 4b) about zero load. This may also be attributed to a sudden rotation of the pins at low load levels (small friction capacity) on an almost straight strut.

## 4. Tests and analysis of unstiffened struts

Four tests on RHS struts are reported here. Section dimensions, initial midspan crookedness and the nominal stresses determined from coupon tests and used in the analysis are shown in Table 1. The initial crookedness was induced by subjecting the specimens to a transverse concentrated load at midspan. The loading schedule was controlled by a limit axial deformation of 3.8 mm. In the folowing analyses, $\lambda$ was taken as 0.01 and $\lambda_y$ as 0.1.

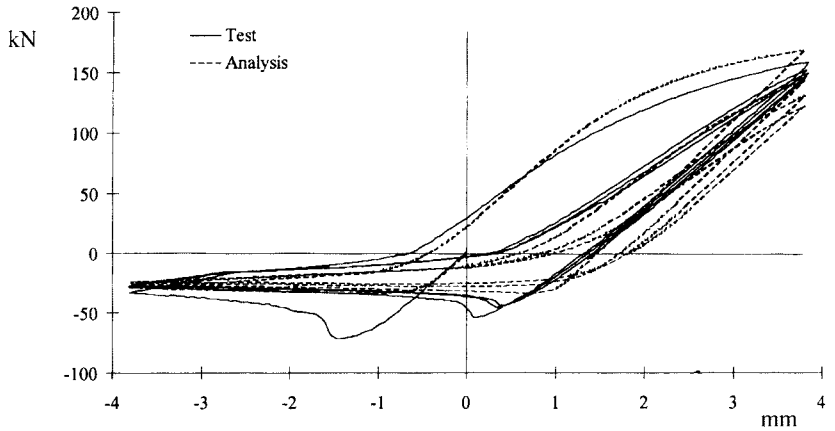


(a) axial load versus axial displacement

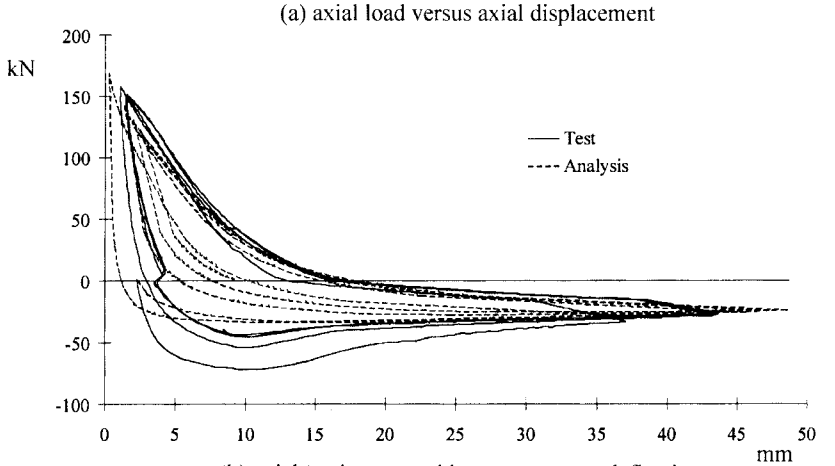


(b) axial load versus midspan transverse deflection

Fig. 4 Test and analysis results for an unstiffened RHS 50×20×3

Test and analytical results for the first four cycles of loading are shown in Figs. 4 to 7 for the four cases in Table 1. The figures show the axial loads versus axial displacement and transverse midspan deflections. The first compression peaks are underestimated by the analysis probably due to friction

Table 1 Dimensions and properties of the unstiffened struts

| Section breadth×height ×wall thickness [mm] | Span (mm) | Initial crookedness $D_1$ (mm) | Yield stress $\sigma_y^o$ (MPa) | Ultimate stress $\sigma_u^o$ (MPa) | Slenderness ratio $\left(\frac{\text{Span}}{\text{Radius of gyration}}\right)$ |
|---|---|---|---|---|---|
| 50×20×3 | 1099 | 2.28 | 220 | 425 | 113 |
| 50×25×2.5 | 1100 | 1.7 | 220 | 425 | 111 |
| 65×35×3 | 1098 | 2.1 | 250 | 500 | 78 |
| 75×25×2.5 | 1100 | 1.725 | 275 | 525 | 107 |

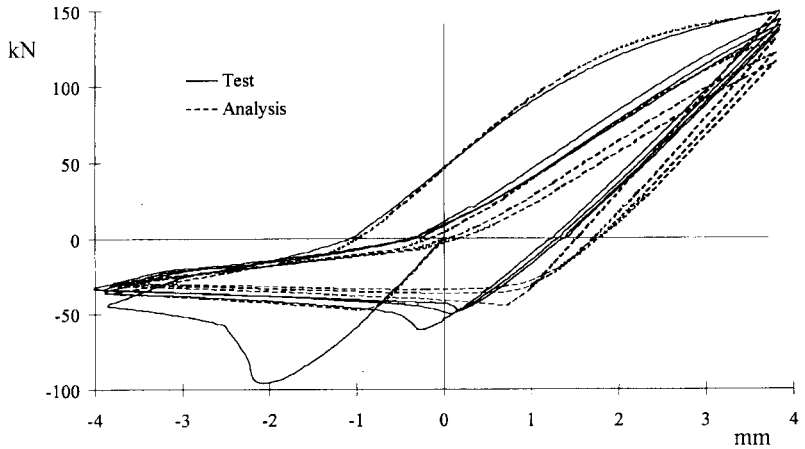


(a) axial load versus axial displacement

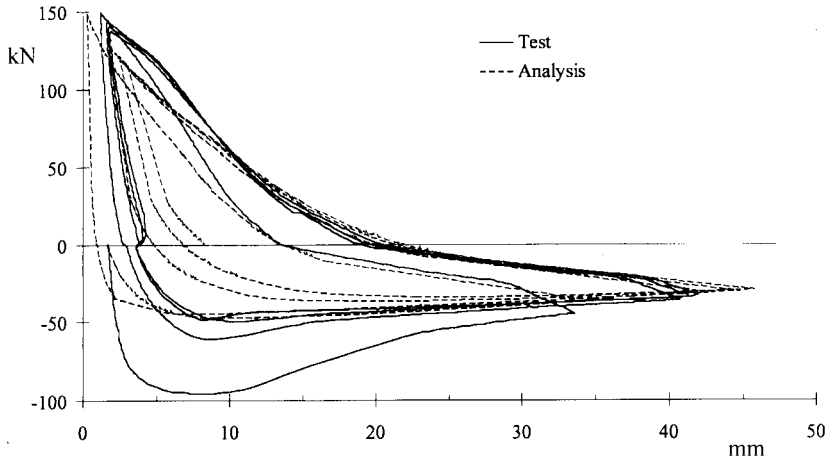


(b) axial load versus midspan transverse deflection

Fig. 5 Test and analysis results for an unstiffened RHS 50×25×2.5

of the end pins as mentioned above. However, tests and analyses converge after the initial sudden drop in load. The results for loads and deflections at the end of the compression strokes are in good agreement especially for the load versus axial displacements. These results are important for the analysis of braced frames and for the evaluation of structural (hysteretic) damping. It is also noted that in the case of RHS 65×35×3, where the sudden drop in midspan deflection at load reversal during unloading from tension is small (Fig. 6b), a very good agreement in the results of load versus transverse deflections is achieved. This was due to its being the stiffest specimen (of lowest slenderness ratio) and thus required the largest restraining end moments (exceeding friction). This supports the earlier conclusion that discrepancies are strongly related to friction.

The main difference during tension strokes is the analysis' prediction of lower permanent deflections (or larger plastic recovery) at the end of the first tension strokes compared to the tests. Also, the spread of extreme tension loads is generally larger in the analyses than in the tests. These discrepancies may also be attributed to end friction as the pins are subjected to large loads and, consequently, large friction couples in later stages of tension. No local buckling was observed in

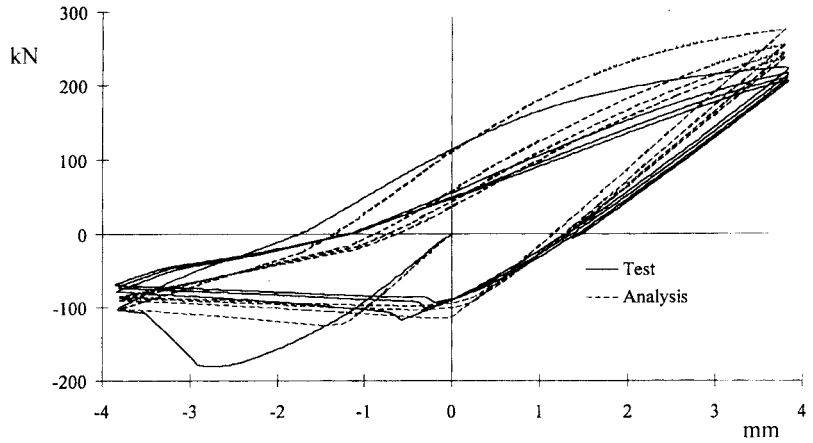


(a) axial load versus axial displacement

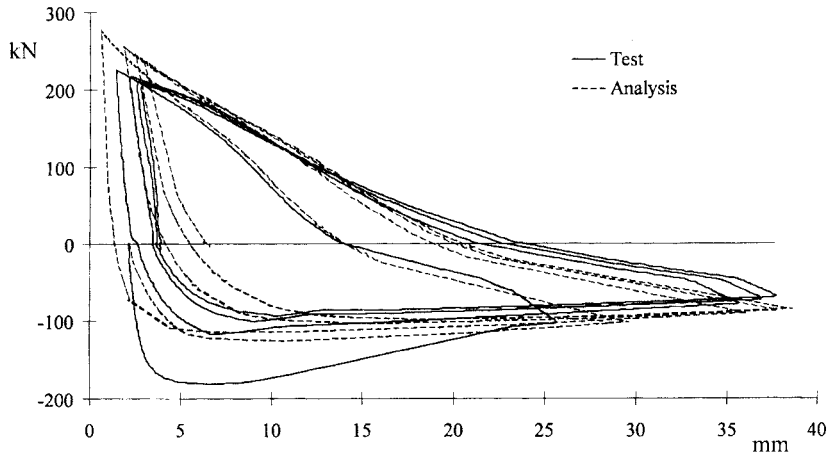


(b) axial load versus midspan transverse deflection

Fig. 6 Test and analysis results for an unstiffened RHS 65×35×3

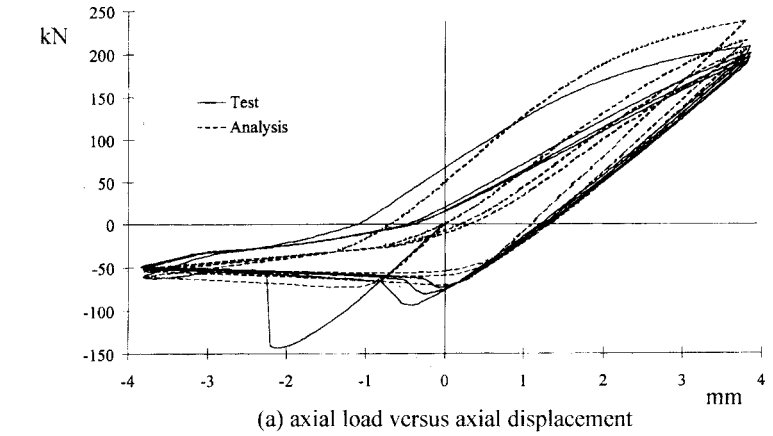


(a) axial load versus axial displacement

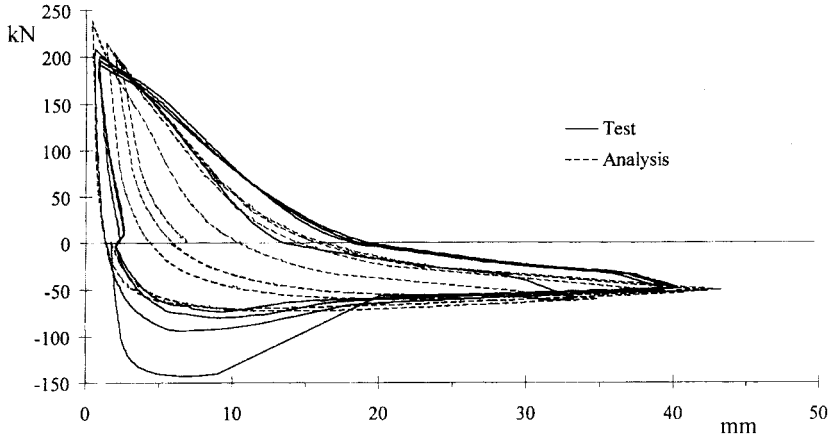


(b) axial load versus midspan transverse deflection

Fig. 7 Test and analysis results for an unstiffened RHS 75×25×2.5

any of the four tests.

## 5. Tests and analysis of stiffened struts

Five crooked RHS struts were tested after stiffening their middle portions. Prior to stiffening, the specimens were initially cyclicly loaded as per the schedule above. Rectangular plates were welded along the webs (shorter sides) of the crooked struts. The midheight of the patch plates coincided with those of the original members at the two quarter points of the plates (Fig. 8). RHS section and stiffener dimensions and the initially induced midspan crookedness are shown in Table 2 where the nominal stiffener lengths are specified as ratios of the strut spans. The actual length of the plate was 70 mm longer to allow for 35mm stress transfer length at each end of the plate. The stiffening plates were made of steel grade 350 as the RHS sections with offset yield stresses of 325 to 425 MPa. In the analyses below they were considered to be of the same material as the original RHS to which they were welded (Table 1). In order to increase the bending stiffness of the strut, deep stiffeners were required. An initial analysis showed that the original webs of RHS have negligible effect on

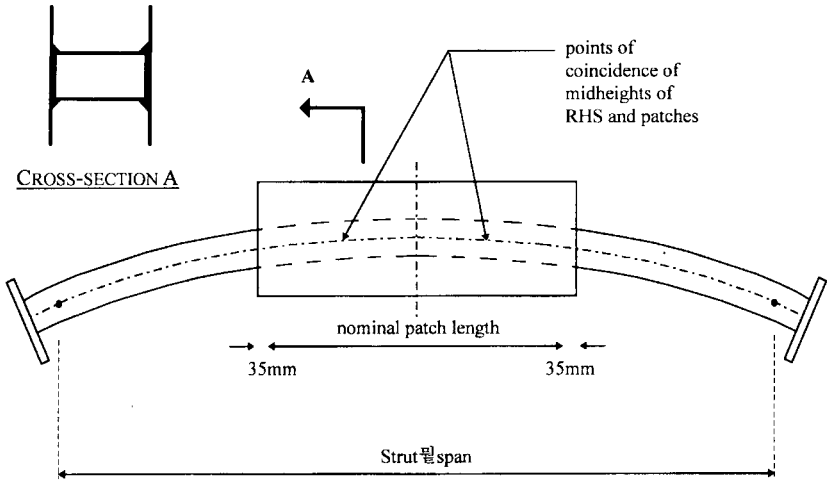


Fig. 8 Details of a stiffened strut

Table 2 Dimensions and properties of the stiffened struts

| Test | Sections breadth×height ×wall thickness | Span (mm) | Nominal patch length (ratio of span) | Patch section | Initial crookedness $D_1$ (mm) |
|---|---|---|---|---|---|
| 1 | 50×20×2 | 1093 | 0.5 | 50×2 | 16 |
| 2 | 65×35×3 | 1093 | 0.5 | 70×2 | 30 |
| 3 | 65×35×3 | 1091 | 0.6 | 50×4 | 27 |
| 4 | 75×25×2.5 | 1091 | 0.5 | 70×4 | 26 |
| 5 | 75×25×2.5 | 1096 | 0.6 | 50×4 | 25 |

the stiffness of the cross-section in the stiffened zones. The webs of the original section were omitted in the analysis of the stiffened zones. Their contribution to the elastic bending stiffness of the cross-section was accounted for by increasing the area of each flange by a third of a web area. Consequently, the total area of the cross-section is reduced by two thirds of the web cross-sectional area. Before application of the stiffeners, each of the initial cyclic loading schedules (similar to those for cyclic loading above) ended with a compression stoke. The resulting current cyclic yield stresses for compression were larger than the nominal yield stresses. However, because stress relation in Eq. (1a) is initially steep and tangential to the linear-elastic line, the variations of the yield stresses were neglected. Both patch plates and RHS sections were assumed to yield at the nominal yield stresses of the RHS (Table 1). The effect of this approximation was discussed in the context of comparing between quasi-kinematic and isotropic hardening (Boutros 2000). The moduli of elasticity of the patched RHS struts were reduced to 190 GPa.

The first specimen, RHS 50×20×2, did not experience local buckling either before or after stiffening. The stiffened strut buckled mildly in an overall mode after the peak load. The concave flanges of the other four specimens buckled slightly about midspan during a late cycle of the initial loading. Their stiffeners also buckled during unloading from the peak compressive load. It does not seem that in any of these four later cases the peak value was influenced by buckling of the

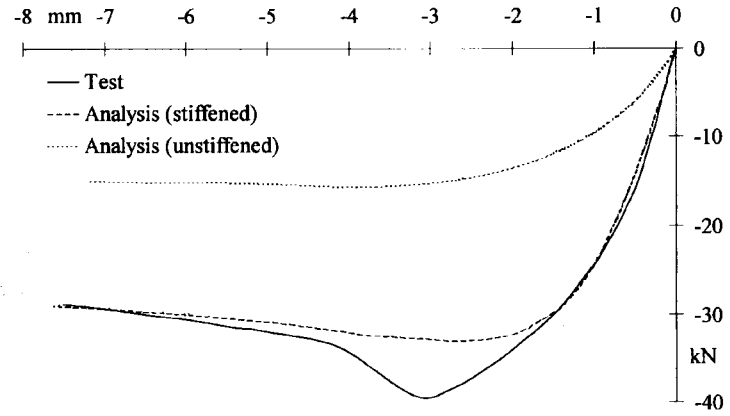


Fig. 9 Axial force versus axial displacement of a stiffened 50×20×2 strut Test 1: 50×2 plate over 0.5 of the span

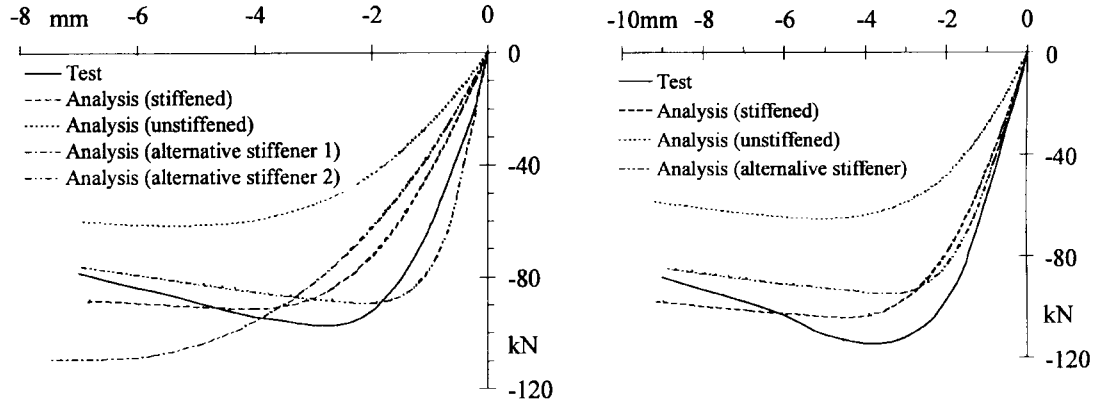


(a) Test 2: 70x2 plate over 0.5 of the span
Alternative stiffener 1: 50x2 over 0.7 of span
Alternative stiffener 2: 140x4 over 0.25 of span

(b) Test 3: 50x4 plate over 0.6 of the span
Alternative stiffener: 60x4 over 0.5 of span

Fig. 10 Axial force versus axial displacement of stiffened 65×35×3 struts

stiffeners for which the maximum outstand width to thickness ratio was less than 9:1.

Due to the retrofitting procedure and the eccentricity of the patching plates with respect to the original struts, the net eccentricity of the centroid of the cross-sections with respect to the straight loading line was discontinuous and coincided with midheight at its quarter points (the points of reference) only.

Test and analysis results of these cases are shown in Figs. 9 to 11 along with the analytical responses of the respective damaged unstiffened struts. The figures show that the analysis predicts adequately the test results. They also reflect the increase in strength achieved by stiffening. Discrepancies after the peak loads of tests 2 to 5 are attributed to local (plate) buckling which was not considered in the analysis. It is worth noting the absence of the compression peaks observed earlier in the tests on prismatic struts (Figs. 4 to 7) because of the larger initial crookedness of the retrofitted struts. The analytical responses are more flexible than the experimental results due to the

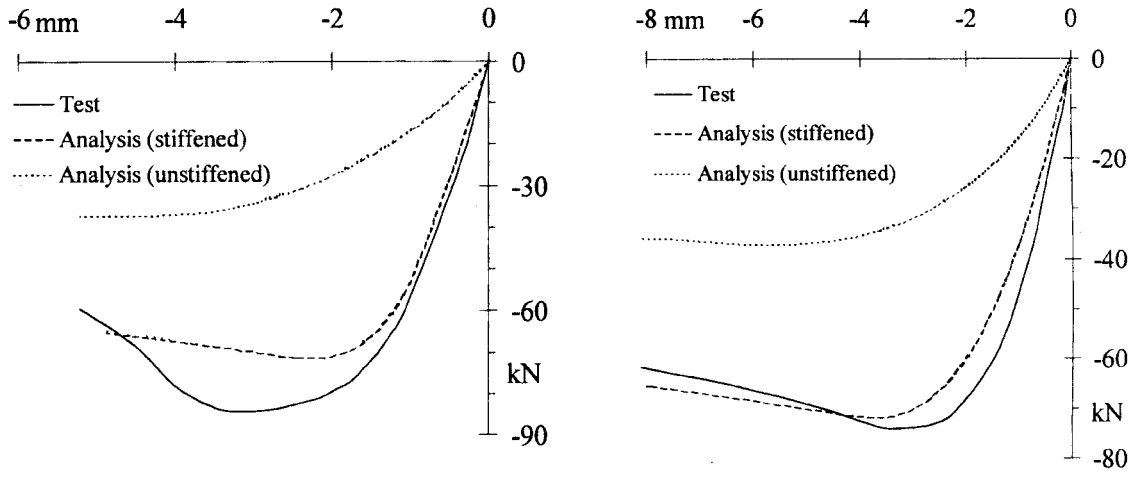


(a) Test 4: 70x4 plate over 0.5 of the span (b) Test 5: 50x4 plate over 0.6 of the span

Fig. 11 Axial force versus axial displacement of stiffened 75×25×2.5 struts

reduced area of the original RHS section in the stiffened region and due to the overestimation of the midspan eccentricity in the analysis. As mentioned above, the latter was taken as the crookedness of the original section and the stiffeners were assumed to be concentric with it; which does not strictly correspond to the stiffener's geometry.

Fig. 10 shows, along with the response of the test stiffeners, analytical responses of alternative stiffeners of the same volume (alternative 1 in test 2, and the alternative in test 3). In both cases, the longer patch resulted in a higher strength of the stiffened strut. This is due to the higher bending stiffness of the struts with longer stiffeners that resulted in a reduction of transverse deflections and, consequently, of bending moments. In general, a longer patch is more efficient than a shorter one. Fig. 10(a) shows also a second alternative of double the volume but of half the length of the test case. In this case, yield of the stiffening plates was delayed but the resulting overall strength of the strut was smaller than the test case. Also, this alternative exhibits a steeper drop in load after the peak than the other two cases (Fig. 10a). Applying very stiff short patches may result in increasing the strength of the stiffened strut to the point where it buckles suddenly with a large drop in load as in test 1 (Fig. 9). This results in a reduction in its energy dissipation capacity. The analysis of test 1 showed that, soon after reaching the peak load, midspan permanent crookedness increased rapidly resulting in the yield of the stiffeners.

Material and geometric conditions of a damaged brace need to be carefully assessed in order to design stiffeners. The required material properties are nominal yield and ultimate stresses. It was shown that the current hysteretic yield stress at different cross-sections is of little effect on the results of the analysis. Instead the nominal yield value may be used. The main geometric property of a pinned strut is its midspan permanent deflection. A damaged brace in a building frame would be subjected to an initial force at rest. This force would usually be tensile in a singly braced frame because the brace would undergo larger deformation strokes in compression than in tension. Then, the measured crookedness would be much smaller than the real one of the unloaded strut. Due to the sensitivity of the response to the initial crookedness of the unloaded strut, it is necessary to estimate it accurately or, conservatively, to overestimate it.

## 6. Conclusions

Prismatic and retrofitted RHS pinned struts were tested. Retrofitting was achieved by welding stiffening plates along the webs of damaged struts. Material properties followed a quasi-kinematic hardening hysteresis path as observed from coupon tests. The analytical and experimental results were compared showing a good agreement for both standard and retrofitted struts. It confirmed that partial plasticity should be considered for this level of deformations (less than 5 times the axial yield displacement). Alternative stiffener dimensions were discussed showing that more efficient strengthening is achieved by using long thin stiffeners rather than short thick ones.

## References

Boutros, M.K. (2000), "Inelastic behavior of standard and retrofitted rectangular hollow sectioned struts. II: Analytical model", *Structural Engineering and Mechanics, An Int'l Journal*, **10**(5), 491-504.

Jain, A.K., Goel, S.C. and Hanson, R.D. (1978), "Hysteresis behavior of bracing members and seismic response of braced frames with different proportions." Rep. No. UMEE 78R3, Department of Civil Engineering, The University of Michigan, Ann Arbor, Michigan.

Nonaka, T. (1989), "Elastic-plastic bar under changes in temperature and axial load" *J. Struct. Engrg., ASCE*, **115**(12), 3059-3075.

## Notation

| | |
|---|---|
| $D_1$ | crookedness at mid-span |
| $D_2$ | elastic deflection at mid-span |
| $E$ | modulus of elasticity |
| $\varepsilon$ | strain |
| $\varepsilon_y^o$ | initial (nominal) yield strain |
| $\varepsilon_y^c$ | incremental yield strain of the current stroke |
| $\lambda$ | final slope of the plastic stress-strain curve (ratio of $E$) |
| $\lambda_y$ | hysteresis parameter (dimensionless) |
| $\sigma$ | stress |
| $\sigma^c$ | current stress before unloading |
| $\sigma_y^o$ | initial (nominal) yield stress |
| $\sigma_u^o$ | nominal ultimate stress |
| $\sigma_y^c$ | yield stress at the start of the current yield stage |

### Superscripts

| | |
|---|---|
| $o$ | initial (nominal) value |
| $c$ | current value |

### Subscripts

| | |
|---|---|
| $u$ | ultimate |
| $y$ | yield |